

# Magnetization transfer imaging in multiple sclerosis

*Matteo Mancini and Mara Cercignani*

Cardiff University Brain Research Imaging Centre, Cardiff University, Cardiff, Wales,  
United Kingdom

## O U T L I N E

<b>Introduction</b>	192	<i>Normal-appearing white matter</i>	198
<i>History</i>	192	<i>Gray matter</i>	199
<i>Magnetization transfer experiment</i>	192		
<b>Clinical use of magnetization transfer contrast</b>	193	<b>Quantitative magnetization transfer in multiple sclerosis</b>	200
<b>Quantifying the magnetization transfer effect</b>	193	<b>Magnetization transfer saturation in multiple sclerosis</b>	200
<i>Magnetization transfer ratio</i>	194	<b>Inhomogeneous magnetization transfer in multiple sclerosis</b>	200
<i>Quantitative magnetization transfer models</i>	194	<b>Magnetization transfer in spinal cord and optic nerve</b>	201
<i>Magnetization transfer saturation</i>	196	<i>Spinal cord</i>	201
<i>Inhomogeneous magnetization transfer</i>	197	<i>Optic nerve</i>	201
<b>Validation of magnetization transfer–derived parameters as myelin markers</b>	198	<b>Conclusions</b>	202
<b>Magnetization transfer ratio in multiple sclerosis</b>	198	<b>References</b>	202
<i>Lesions</i>	198		

---

## Introduction

---

Magnetization transfer (MT) refers to the exchange of magnetization occurring between spins sitting in different molecular environments. This exchange means that any external interaction with one of the two proton pools results in changes to the other pool. As protons attached to large molecules are typically “magnetic resonance imaging (MRI)–invisible” due to their short  $T_2$ , MT can be exploited to indirectly probe them.

### History

The ability of nuclei in *different molecular compounds* to exchange magnetization was first demonstrated using nuclear magnetic resonance (NMR) spectroscopy in a system consisting of two weakly coupled sets of spins [1]. The concept was later extended to protons with the same resonant frequency and different transverse relaxation time  $T_2$  [2], such as water protons and macromolecular protons in collagen or muscle. This phenomenon is typically explained as follows: the relatively “immobile” macromolecular protons produce a signal that decays too fast to be detected with standard MR sequences. This is due to their very short  $T_2$ , which causes their signal to decay faster than the typical echo times achievable on a clinical scanner. In biological tissue, macromolecular protons are mainly found in lipids and proteins. Water protons, by contrast, are the main contributors to the signal typically visible on magnetic resonance imaging (MRI). They are in constant motion, and when they come in contact with macromolecular protons, they can exchange magnetization with them. Through this magnetization exchange, the magnetization state of the water pool protons can affect that of the macromolecular protons, and vice versa. The myelin bilayer is made up of approximately 80% lipid and 20% protein [3], which makes MT of great relevance for the study of demyelinating disorders. In 1989, magnetization transfer *imaging* was introduced by Wolff and Balaban [4].

### Magnetization transfer experiment

There are different ways of probing MT, but the simplest one relies on the differently shaped resonance lines of water (liquid pool) and macromolecular protons (Fig. 11.1). The width of such lines is inversely proportional to the protons  $T_2$ , and therefore macromolecular protons tend to have much broader line shape than water protons. This property can be exploited to selectively interact with the macromolecular proton pool by using radio frequency (RF) pulses tuned few kilohertz (kHz) away from the central resonance frequency (also known as *off-resonance* pulses). These pulses “saturate” the macromolecular pool, that is, cause the number of up-spins and down-spins to be the same, thus nulling the magnetization vector for the macromolecular protons. This saturation can be partially transferred to the liquid protons via MT, thus reducing the measured MRI signal (see Fig. 11.1). The resulting attenuation depends on the density of macromolecular protons and their ability to exchange magnetization. As a consequence, tissues with higher concentration of macromolecules will appear darker than tissues with primarily liquid content. This phenomenon creates a source of contrast in MRI which is independent from  $T_1$  and  $T_2$ , and, importantly, is sensitive to the myelin content in the brain.

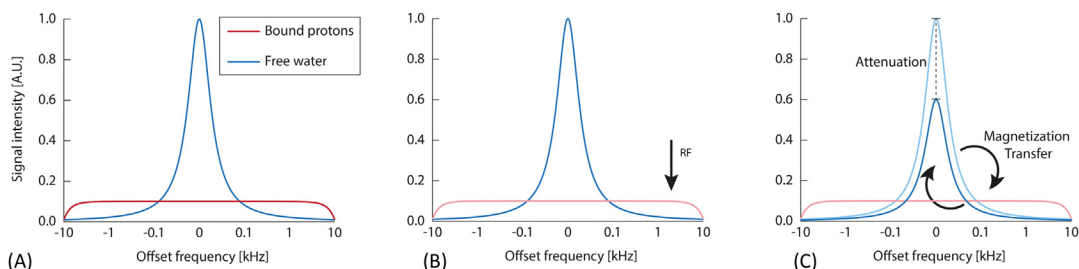


**FIGURE 11.1** Qualitative representation of the spectra of free water and bound protons before and after RF irradiation. The spectra of the two pools are centered around the same frequency, but the free water protons present a narrow line shape (blue), while the macromolecular protons (red) present a broad line shape (A). If an RF pulse is applied with a frequency offset larger than 1–2 kHz, the free water pool is unaffected, while the macromolecular pool magnetization is saturated (B). As a result of the magnetization transfer between macromolecular protons and free water, the saturation is partially transferred to the latter pool, and attenuates the signal from the water itself (C).

In the early NMR experiments, off-resonance saturation was achieved using the so-called continuous wave irradiation, that is, applying constant RF energy for a long period (typically of the order of 1 second) with relatively low power, using a second transmitter system. Due to large power deposition into the patient, this method is not practical or safe for clinical use, and requires dedicated hardware, not available as standard on clinical MRI equipment. For this reason, on human MRI scanners, the so-called *pulsed MT* is used [5]. In this case, regular RF pulses (similar to those used for excitation and refocusing but typically larger) are used. They are tuned a few kHz (usually 1–2 kHz) from the resonant frequency and occur at regular intervals so that their effect can add up and create sufficient saturation. MT modules can be added to almost any MRI sequence, but they are most commonly used in spoiled gradient echo (fast low angle shot [FLASH], spoiled gradient-recalled [SPGR]) for efficiency. Alternative approaches to probe the MT effects rely on on-resonance saturation [6,7].

### Clinical use of magnetization transfer contrast

MT increases the contrast between tissues rich in macromolecular content and fluids. This feature finds applications both in the brain and the body. Examples include musculoskeletal imaging (to provide increased contrast between cartilage and synovial fluid) and time-of-flight MRI angiography, where it helps to suppress background tissue [8]. In conjunction with gadolinium injections, it can improve the visibility of gadolinium-enhancing lesions [9].

### Quantifying the magnetization transfer effect

The sensitivity of MT MRI to myelin density in the brain quickly attracted the interest of researchers in the field of multiple sclerosis (MS). The availability of a noninvasive technique potentially able to quantify the degree of demyelination clearly offers great

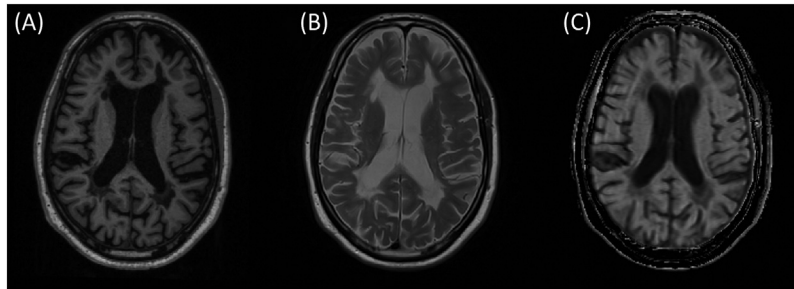


**FIGURE 11.2** T1-weighted (A), T2-weighted (B), and magnetization transfer ratio (MTR) (C) images of a patient with secondary progressive multiple sclerosis (MS). Demyelinating lesions can be clearly seen on all scans, and they appear as hypointensities on the MTR map. In this example, the MTR of the normal appearing white matter ranges between 39 and 46 percentage units (p.u.), while the average values within lesions ranges between 17 and 28 p.u.

potential, and also the challenge of developing suitable methods to translate MT contrast into a quantitative and meaningful measurement. Increasingly complex approaches were proposed over the years, with variable degree of requirements in terms of specialized software and scan time.

### Magnetization transfer ratio

The simplest approach proposed to quantify the MT effects in biological tissues is the magnetization transfer ratio (MTR). To compute MTR, only two proton-density acquisitions are required, one with an off-resonance saturation pulse and the other without. From the resulting images, MTR is then calculated pixel-wise using the following formula:

$$\text{MTR} = \frac{M_0 - M_s}{M_0} \cdot 100$$

where  $M_s$  and  $M_0$  refer, respectively, to the images acquired with and without saturation. An example of an MTR map is shown in Fig. 11.2 (panel C). Each voxel in the resulting MTR map will contain a value from 0 to 100, providing a measure of the related macromolecular content. In brain imaging, the cerebrospinal fluid (CSF) will show values close to zero—because of the absence of macromolecules—while white and gray matter areas will show values depending on the acquisition parameters, with white matter showing higher MTR than gray matter. The drawbacks of this very simple approach are (1) the lack of a direct and clear biological or physical interpretation [10], and (2) the dependency on the acquisition parameters, in particular the magnetic field strength [11], the off-resonance pulse characteristics [12], and both the repetition time and flip angles [13].

### Quantitative magnetization transfer models

To overcome the limitations of MTR, it is necessary to analytically describe the MT phenomena. With this goal in mind, the methods developed for quantitative

magnetization transfer (qMT) leverage compartment modeling to formulate and fit the physical parameters underlying those phenomena. Historically, the first qMT method has been developed by Henkelman et al. [14] for continuous wave RF irradiation experiments using agar gels. In these experiments, the system under study is composed of two compartments or pools: the liquid pool (A) and the macromolecular pool (B). Each pool can be described by the density of spins ( $M_0^A$ ,  $M_0^B$ ) and the proportion of saturated spins, which depends on the past irradiation phenomena. The irradiation itself also causes multiple magnetization modifications and exchange phenomena—specifically, after the irradiation pulse:

- T1 relaxation causes the longitudinal magnetization of both pools to increase (with relaxation rates  $R_A$  and  $R_B$ , respectively);
- absorption of off-resonance irradiation counteracts T1 relaxation by saturation and therefore reducing the longitudinal magnetization (with rates  $R_{RFA}$  and  $R_{RFB}$ );
- the two pools exchange magnetization with rate constant  $R$ , which results in the superposition of the exchanges  $A \rightarrow B$  (with rate  $R_{M0B}$ ) and  $B \rightarrow A$  (with rate  $R_{M0A}$ ).

Coupled Bloch equations can then be written for this system that combines all these different effects. In the continuous wave regime adopted by Henkelman et al., this system can be fully described by solving analytically in the steady state the coupled Bloch equations (for a detailed derivation see Cercignani et al. [15]), providing estimates of each pool's parameters. As mentioned, continuous wave experiments are not viable for clinical applications, and unfortunately pulsed MT experiments would require a numerical approach to solve the same equations, which is computationally expensive. For this reason, several approximations have been proposed for the two-pool model in pulsed regime [16–18].

Fitting the two-pool model pixel-wise results in five different parameter maps: the macromolecular pool fraction; the transverse relaxation times for each pool ( $T_{2A}$  and  $T_{2B}$ ); the pseudo-first-order exchange rates between the pools ( $RM_{0A}$  and  $RM_{0B}$ , also known as  $k_f$  and  $k_r$ , respectively). Among these maps, the one that has received the most attention is the macromolecular pool fraction, as it has been shown to reflect myelin content [19]. Fig. 11.3 shows the main parametric maps derived from qMT.

The fundamental assumption of the two-pool model is that there is a single compartment of water. This is not the case in brain tissue, where water molecules can belong to the intra- and extra-cellular space, or be trapped in the myelin sheath wrapping around the axons. It is interesting to notice that a different quantitative MRI approach aiming at quantifying myelin, namely  $T_2$  relaxometry, offers a complementary perspective: in  $T_2$  relaxometry, one can estimate the size of the intra/extra-cellular and myelin water compartments, at the cost of neglecting the magnetization exchange between pools. A combination of these two approaches, resulting in a four-pool model, has been proposed [20,21], but the number of parameters to be estimated imposes extremely long scan times, which do not make it a viable approach for clinical applications.

Another important issue to keep in mind is related to partial voluming effects: as the spatial resolution for qMT acquisitions can go from 1 to 3 mm, the presence of CSF in a voxel can introduce a bias in the fitting, as the MT effect in CSF is negligible. To overcome this issue, Mossahebi et al. [22] have proposed a three-pool model, where the third pool represents a nonexchanging water compartment and takes into account CSF contributions.

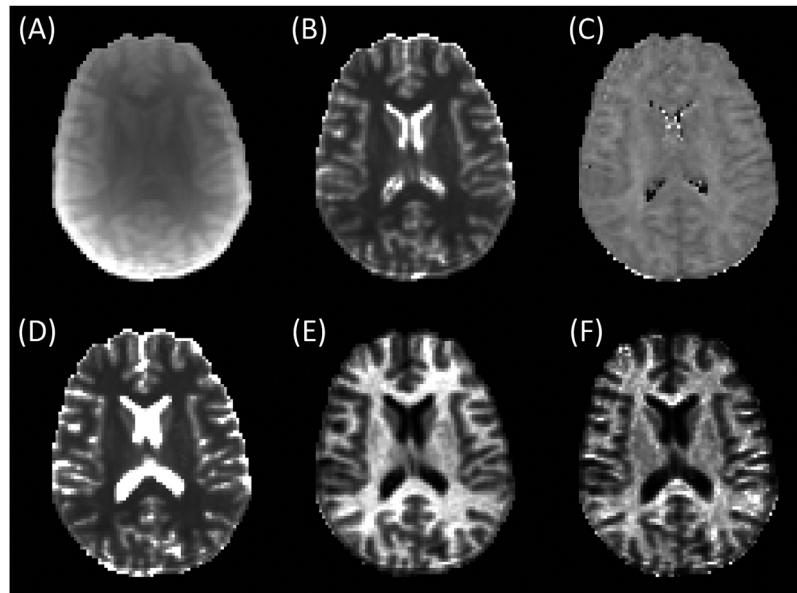


FIGURE 11.3 Quantitative magnetization transfer (MT) parametric maps derived from fitting an approximation of Henkelman's model to human brain data. Proton density (A),  $T_{1A}$  (B),  $T_{2B}$  (C),  $T_{2A}$  (D), F (E), and  $RM_{0A}$  (F).

Arguably, the main drawback limiting a wider use of qMT is the long acquisition time required. To overcome this drawback, Yarnykh and Yuan have proposed additional constraints to shorten the overall acquisition [23]. The same group also proposed a reduced protocol (consisting of one MT-weighted measurement and a reference scan) to estimate exclusively the macromolecular pool fraction [24,25].

### Magnetization transfer saturation

In order to overcome the limits of MTR and keep at the same time a relatively shorter acquisition time compared to qMT, a different method focuses on the magnetization transfer saturation ( $MT_{sat}$ )—a phenomenological parameter with no biophysical meaning, but overcoming some of the main shortfalls of MTR. As proposed by Helms et al. [13], this approach leverages a protocol that requires three commonly available acquisition sequences (T1-weighted, PD-weighted, MT-weighted) and allows to estimate not only  $MT_{sat}$  but also the longitudinal relaxation time  $T_1$  and the apparent proton density. Despite lacking a direct biological interpretation,  $MT_{sat}$  inherently corrects for  $T_1$  relaxation and on-resonance excitation phenomena. It should be remarked that changes to the acquisition sequence will result in changes to the estimated  $MT_{sat}$ .

This approach has become increasingly popular in the last year, and a contributing factor for its popularity was the release of multiparameter mapping (MPM) protocols and processing tools from Weiskopf and colleagues [26,27]. The MPM protocols also include

solutions based on vendor sequences already available in MRI scanners (<https://hmri-group.github.io/hMRI-toolbox/>), bypassing the need for tailored sequence development.

## Inhomogeneous magnetization transfer

Inhomogeneous magnetization transfer (ihMT) was reported for the first time in 2005 [28] as an incidental finding during an arterial spin labeling scan. As explained in the introduction to this chapter, in a typical MT experiment off-resonance pulses are used to saturate the macromolecular pool: such pulses are tuned either at a negative (i.e., few kHz below the Larmor frequency) or a positive (i.e., few kHz above the Larmor frequency) frequency. In the experiment performed by Alsop et al. [28], instead, pulses with power evenly split between positive and negative frequency offsets (dual-frequency irradiation) were alternated (Fig. 11.4), and the resulting images showed a marked reduction of signal within the white matter, suggesting high specificity for myelin. The prevalent explanation for this augmented specificity is that MT relies on a combination of spin interactions. Some of these effects are negligible in isotropic liquids, but can leave a residual component for protons with a preferential molecular orientation, such as myelin bilayers. The dual-frequency irradiation used for ihMT effectively removes these effects while the single-frequency saturation (used for regular MT) does not. A way of highlighting such effects is therefore to compare images obtained with the two types of irradiation. An inhomogeneous magnetization transfer ratio (ihMTR) map is computed by obtaining images with positive ( $MT_+$ ), negative ( $MT_-$ ) and dual irradiation ( $MT_{\mp}$ ,  $MT_{\pm}$ ) and then combining them as follows:

$$ihMTR = \frac{(MT_+ + M_-) - (MT_{\mp} + M_{\pm})}{MT_0}$$

where  $MT_0$  is the reference image, without any saturation.

IhMT is still in its infancy and more work is needed to understand its underlying mechanisms, validate it, and develop reliable acquisition techniques that can be translated into clinical applications. Nevertheless, it is a promising approach to improve specificity to myelin.

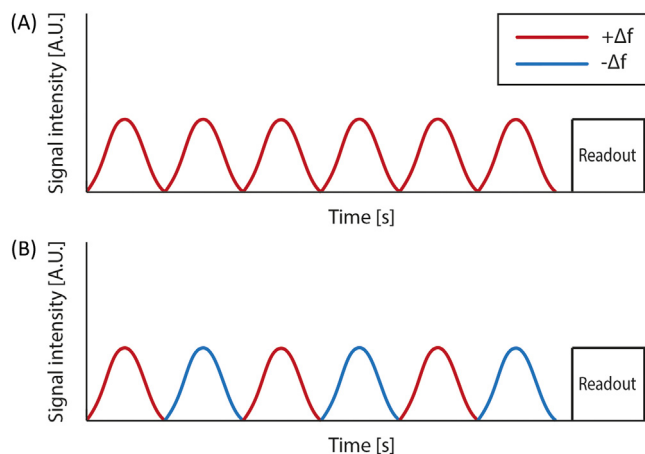


**FIGURE 11.4** A conventional (A) vs inhomogeneous (B) MT experiment. In the former case, the MT pulses are all tuned at the same offset frequency, while in the latter case, positive and negative offsets are alternated.

## Validation of magnetization transfer–derived parameters as myelin markers

Several studies have attempted to establish the relationship between histological measures of myelin and quantities derived from MT techniques. Both rodent and postmortem human studies have confirmed a moderate association between MTR and myelin content [29,30]. The macromolecular pool fraction derived from qMT also showed good correlation with myelin content in experimental models of both, demyelination and remyelination [31–33]. However, it is known that MT-derived parameters also correlate with edema and inflammation. In experimental allergic encephalomyelitis, MTR decreases were reversed with suppression of inflammation [34]. Correlations with the number of inactive macrophages within lesions, and with other indices of inflammation have also been reported [35]. These findings are not surprising, as the MTR measures a ratio between macromolecular and water protons, and therefore changes to its value are driven by changes to both pools. Despite these limitations, a recent meta-analysis [19] has confirmed that MT-based measures have the highest correlations with myelin content among all the MRI techniques that have been proposed as proxies of myelin.

## Magnetization transfer ratio in multiple sclerosis

### Lesions

Reductions in the MTR were observed from the early days within MS lesions [5,36,37], consistent with demyelination. A variable range of MTR values can be found in lesions (see Fig. 11.2 for an example), with lower values in lesions appearing as hypointense on T1-weighted scans [38]. The lower MTR typically observed in T1-hypointense lesions is consistent with the recognition that these so-called “black holes” are the fraction of lesions with the most severe axonal loss and demyelination. Longitudinal MTR assessments have shown rapid changes over time in newly enhancing lesions. Dramatic reductions in MTR at lesion appearance have been consistently reported [39]. Within these lesions, the MTR tend to recover, at least partially, over a few weeks. Such rapid changes suggest that the initial drop might be driven by an increase in water content due to edema, rather than by a reduction in myelin. Conversely, persistent MTR reductions after 3–6 months suggest a substantial loss of myelin [40] and the presence of permanent tissue damage (see Fig. 11.5). MTR reductions have also been detected retrospectively in the normal-appearing white matter (NAWM) before lesion formation [41,42]. These changes in MTR are probably explained by a combination of edema and gliosis, followed by demyelination. In ring-enhancing lesions, the lowest MTR values are typically found in the center, where myelin loss is likely to have occurred, while inflammatory processes are taking place at the periphery [38,43].

### Normal-appearing white matter

Although the MTR is typically larger in the NAWM compared to T<sub>2</sub>-hyperintense lesions, abnormally low MTR values are found also in the NAWM compared to the white matter of

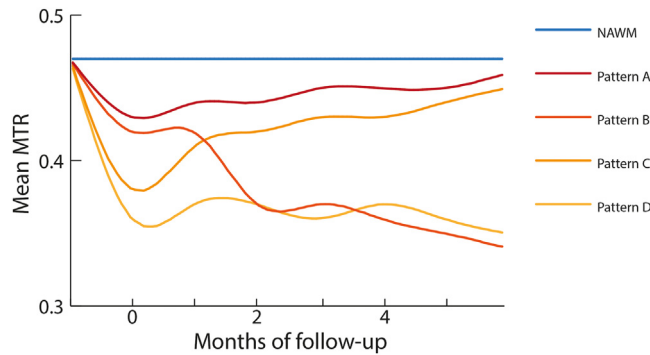


**FIGURE 11.5** MTR value evolution in active MS lesions from appearance over 6 months of followup. The four lines correspond to lesions showing different patterns of appearance on T1-weighted images: pattern A (dark red), initially isointense lesions remain isointense; pattern B (light red), initially isointense lesions become hypointense; pattern C (orange), initially hypointense lesions become isointense; and pattern D (yellow), initially hypointense lesions remain hypointense. Note the “dip” in MTR occurring approximately at lesion appearance (month 0). Source: Adapted with permission from van Waesberghe JH, van Walderveen MA, Castelijns JA, Scheltens P, Lycklama à Nijeholt GJ, Polman CH, et al. Patterns of lesion development in multiple sclerosis: longitudinal observations with T1-weighted spin-echo and magnetization transfer MR. *AJNR Am J Neuroradiol* 1998;19(4):675–83.

healthy controls [5], with typically decreasing values approaching T2-visible lesions [44]. MTR reductions in the NAWM tend to be more widespread in secondary progressive multiple sclerosis (SPMS) than relapsing–remitting multiple sclerosis (RRMS) [45], and not uniform within the white matter. Specifically, a gradient of decreasing MTR toward the ventricles was demonstrated [46], with greater MTR reductions in SPMS compared with RRMS patients. This finding supports the hypothesis that MS pathology might be linked to CSF-mediated factors [47]. This MTR gradient toward the ventricles can be already observed soon after a clinically isolated syndrome, and is predictive of the development of MS, independently of WM lesions [48], and of further relapses after treatment with alemtuzumab [49]. The interpretation for these MTR changes in the absence of macroscopic lesions is multifaceted: we have already discussed how low MTR values can be retrospectively identified in the NAWM before the appearance of a lesion—some studies have reported changes appearing up to 1.5 years before the lesion appears [42]. However, low MTR values can also result from diffuse changes, including edema, gliosis, and myelin thinning. The recurring finding of lower MTR closer to visible lesions [44,50] suggests that it may be caused by a combination of secondary events, including retrograde degeneration.

## Gray matter

MTR was also one of the first quantitative approaches used to assess tissue damage induced by MS to the gray matter, showing reduced values in the gray matter of people with MS, including those minimally disabled [51]. As gray matter lesions are frequent in MS [52] but almost MRI-invisible (particularly in the cortex), access to a quantitative technique able to assess tissue integrity is of great value. Reduced MTR can also be

explained by subtle diffuse pathology or by a combination of both. Several studies of gray matter MTR were conducted in primary progressive multiple sclerosis (PPMS), as typically these patients have lower white matter lesion load but greater disability than people with RRMS. In PPMS, MTR reductions in the gray matter are more widespread than localized atrophy and correlate well with clinical scores [53]. In a longitudinal study in a PPMS cohort, baseline gray matter MTR best predicted progression over 3 years [54]. One potential confound when measuring cortical MTR is partial volume with CSF, which might produce artificially low value in patients with MS then in healthy controls, as they are more likely to show cortical atrophy. It is therefore recommended to adjust for this effect. With recent advances in image analysis more sophisticated approaches have become available, and it was shown that, just like in the NAWM, MTR is not uniform across the cortex: when segmenting the cortex into outer and inner bands, Samson et al. demonstrated a decrease in outer cortical MTR of SPMS and RRMS patients compared to healthy controls, which was not observed in PPMS [55]. This finding could reflect subpial pathology [52].

### Quantitative magnetization transfer in multiple sclerosis

qMT studies in clinical populations have been limited so far, primarily due to the relatively long scan times, and the lack of off-the-shelf acquisition protocols and image analysis packages. Although the latter issue has been partially addressed (notable open-source projects include: qMRLab—<https://qmrlab.org>; and QUIT—<https://quit.readthedocs.io>), commercial sequences for qMT are not yet available. Nonetheless, initial, proof-of-concept studies have shown that the macromolecular pool size ratio,  $F$ , is decreased in lesions and NAWM, as expected in the presence of demyelination [56–58]. A recent systematic review provides an overview of the most consistently reported findings when using MTR and qMT in RRMS [59]. Overall, the macromolecular proton fraction ( $F$ ) and the forward exchange rate ( $k_f$ ) appear consistently reduced in lesions compared to the NAWM, and appear sensitive to lesion severity. In the NAWM changes to qMT parameters are more subtle and less reproducible. A study performed at 7 T investigated qMT in cortical gray matter and found a significant reduction in the exchange ratio of MS patients which was strongly correlated with cognitive performance [60].

### Magnetization transfer saturation in multiple sclerosis

One study looking at  $MT_{\text{sat}}$  in MS showed reduced values in both NAWM and gray matter [61]. The  $MT_{\text{sat}}$  within lesions was tightly associated with cognitive scores.

### Inhomogeneous magnetization transfer in multiple sclerosis

As ihMT is a relatively novel approach, most of the work so far has focused on method development. Initial applications to RRMS have demonstrated reduced ihMTR values

within MS lesions compared to the NAWM, and lower values in the NAWM of patients compared to the white matter of healthy controls. The association with clinical disability was consistently stronger for ihMTR than MTR [62,63].

## Magnetization transfer in spinal cord and optic nerve

Quantitative approaches to quantify myelin in the spinal cord and optic nerve are of great relevance for MS research: spinal cord and optic nerve lesions are typically more symptomatic than brain lesions, and correlate better with the degree of physical disability. Nevertheless, implementing reliable techniques for measuring MT effects in these anatomical locations is challenging, due to not only their specific anatomy, but also their tendency to move. The small section of both the cord and the optic nerve call for high spatial resolution, which, on turn, yields reduced signal-to-noise ratio (SNR) and increased motion sensitivity. Additional complications come from the surrounding tissue (bone, fluid, and fat) that may confound the experiment.

### Spinal cord

In the cord, the majority of investigations have focused on the cervical portion. A simple approach for quantification is  $MT_{CSF}$  [64], which quantifies MT effects relative to the CSF signal. The voxelwise signal is normalized to that measured in a given region of interest (ROI) encompassing CSF only, where MT should be zero.  $MT_{CSF}$  showed tract-specific signal abnormalities in the dorsal and lateral columns of the spinal cord in MS patients [65]. One limitation of  $MT_{CSF}$  is its dependency on  $T_1$  and  $T_2$  contrast, which might be altered in the presence of inflammation. Attempts to set up protocols for qMT in the cord have been mainly hampered by the scan time that can quickly become prohibitively long. Attempts to compensate for this problem have initially focused on ROI-based (rather than voxelwise) fit, due to the relatively low SNR. Faster readouts, such as echo-planar imaging offer an attractive alternative and can be combined with reduced field-of-view acquisition [66]. Finally, single-point qMT approaches have been proposed [67]. Even ihMT has been applied to the spinal cord [68], in combination with diffusion tensor imaging but only in healthy volunteers. Two single slices at C2 and C5 were imaged, showing higher ihMTR at C2 compared to C5.

### Optic nerve

Despite the optic nerve being even more challenging than the cord to image, early attempts to measure the MTR of the optic nerve suggested reduced values in patients with MS and optic neuritis compared to healthy controls [69], and moderate correlations with visual evoked potentials. More recently, an approach toward qMT of the nerve has been proposed using Dixon fat–water separation to remove fatty tissue from MT images [70].

Despite these isolated examples, qMT for these structures is limited by technical challenges and long scan times. Optimized acquisitions, as well as approaches based on reduced models allow the scan time to be reduced and/or the precision to be increased.

## Conclusions

MT techniques offer a unique source of contrast and its sensitivity to myelin has been repeatedly demonstrated against histology. Simple approaches such as MTR or  $MT_{\text{sat}}$  make it a feasible approach in clinical population, and the MTR has been included as a secondary outcome in some pharmacological trials. One of the challenges that remain to be addressed is the standardization across scanner models and manufacturers, which limit adoption in the clinic. More complex modeling of the MT phenomenon has the advantage of providing estimates of true biophysical parameters, with a clear biological interpretability. However, they require long scan times, which are hardly implementable in the clinic. A further limitation of MT-derived parameters is its sensitivity to inflammation, which can bias myelin assessments. Despite these limitations, MT remains one of the most promising ways of measuring myelin noninvasively, and the recent introduction of ihMT promises to improve specificity.

## References

- [1] Forsén S, Hoffman RA. Study of moderately rapid chemical exchange reactions by means of nuclear magnetic double resonance. *J Chem Phys* 1963;39(11):2892–901. Available from: <https://doi.org/10.1063/1.1734121>.
- [2] Edzes HT, Samulski ET. The measurement of cross-relaxation effects in the proton NMR spin-lattice relaxation of water in biological systems: hydrated collagen and muscle. *J Magn Reson* (1969) 1978;31(2):207–29. Available from: [https://doi.org/10.1016/0022-2364\(78\)90185-3](https://doi.org/10.1016/0022-2364(78)90185-3).
- [3] Laule C, Vavasour IM, Kolind SH, Li DKB, Traboulsee TL, Moore GRW, et al. Magnetic resonance imaging of myelin. *Neurotherapeutics* 2007;4(3):460–84. Available from: <https://doi.org/10.1016/j.nurt.2007.05.004>.
- [4] Wolff SD, Balaban RS. Magnetization transfer contrast (MTC) and tissue water proton relaxation in vivo. *Magn Reson Med* 1989;10(1):135–44. Available from: <https://doi.org/10.1002/mrm.1910100113>.
- [5] Dousset V, Grossman RI, Ramer KN, Schnall MD, Young LH, Gonzalez-Scarano F, et al. Experimental allergic encephalomyelitis and multiple sclerosis: lesion characterization with magnetization transfer imaging. *Radiology* 1992;182(2):483–91. Available from: <https://doi.org/10.1148/radiology.182.2.1732968>.
- [6] Gochberg DF, Gore JC. Quantitative magnetization transfer imaging via selective inversion recovery with short repetition times. *Magn Reson Med* 2007;57(2):437–41. Available from: <https://doi.org/10.1002/mrm.21143>.
- [7] Bieri O, Scheffler K. Optimized balanced steady-state free precession magnetization transfer imaging. *Magn Reson Med* 2007;58(3):511–18. Available from: <https://doi.org/10.1002/mrm.21326>.
- [8] Edelman RR, Ahn SS, Chien D, Li W, Goldmann A, Mantello M, et al. Improved time-of-flight MR angiography of the brain with magnetization transfer contrast. *Radiology* 1992;184(2):395–9. Available from: <https://doi.org/10.1148/radiology.184.2.1620835>.
- [9] Finelli DA, Hurst GC, Gullapali RP, Bellon EM. Improved contrast of enhancing brain lesions on postgadolinium, T1-weighted spin-echo images with use of magnetization transfer. *Radiology* 1994;190(2):553–9. Available from: <https://doi.org/10.1148/radiology.190.2.8284415>.
- [10] Henkelman RM, Stanisz GJ, Graham SJ. Magnetization transfer in MRI: a review. *NMR Biomed* 2001;14(2):57–64. Available from: <https://doi.org/10.1002/nbm.683>.
- [11] Cercignani M, Symms MR, Ron M, Barker GJ. 3D MTR measurement: From 1.5T to 3.0T. *NeuroImage* 2006;31(1):181–6. Available from: <https://doi.org/10.1016/j.neuroimage.2005.11.028>.
- [12] Martirosian P, Boss A, Deimling M, Kiefer B, Schraml C, Schweser NF, et al. Systematic variation of off-resonance prepulses for clinical magnetization transfer contrast imaging at 0.2, 1.5, and 3.0 Tesla. *Invest Radiol* 2008;43(1):16–26. Available from: <https://doi.org/10.1097/RLI.0b013e3181559949>.
- [13] Helms G, Dathe H, Kallenberg K, Dechent P. High-resolution maps of magnetization transfer with inherent correction for RF inhomogeneity and T1 relaxation obtained from 3D FLASH MRI. *Magn Reson Med* 2008;60(6):1396–407. Available from: <https://doi.org/10.1002/mrm.21732>.
- [14] Henkelman RM, Huang X, Xiang QS, Stanisz GJ, Swanson SD, Bronskill MJ. Quantitative interpretation of magnetization transfer. *Magn Reson Med* 1993;29(6):759–66. Available from: <https://doi.org/10.1002/mrm.1910290607>.

- [15] Cercignani M, Dowell NG, Tofts PS. Quantitative MRI of the brain: principles of physical measurement: principles of physical measurement. 2nd ed. CRC Press; 2018.
- [16] Ramani A, Dalton C, Miller DH, Tofts PS, Barker GJ. Precise estimate of fundamental in-vivo MT parameters in human brain in clinically feasible times. *Magn Reson Imaging* 2002;20(10):721–31. Available from: [https://doi.org/10.1016/S0730-725X\(02\)00598-2](https://doi.org/10.1016/S0730-725X(02)00598-2).
- [17] Sled JG, Pike GB. Quantitative interpretation of magnetization transfer in spoiled gradient echo MRI sequences. *J Magn Reson* 2000;145(1):24–36. Available from: <https://doi.org/10.1006/jmre.2000.2059>.
- [18] Yarnykh VL. Pulsed Z-spectroscopic imaging of cross-relaxation parameters in tissues for human MRI: theory and clinical applications. *Magn Reson Med* 2002;47(5):929–39. Available from: <https://doi.org/10.1002/mrm.10120>.
- [19] Mancini M, Karakuzu A, Cohen-Adad J, Cercignani M, Nichols TE, Stikov N. An interactive meta-analysis of MRI biomarkers of myelin. *eLife* 2020;9:e61523. Available from: <https://doi.org/10.7554/eLife.61523>.
- [20] Levesque IR, Pike GB. Characterizing healthy and diseased white matter using quantitative magnetization transfer and multicomponent T(2) relaxometry: a unified view via a four-pool model. *Magn Reson Med* 2009;62(6):1487–96. Available from: <https://doi.org/10.1002/mrm.22131>.
- [21] Stanisz GJ, Kecojevic A, Bronskill MJ, Henkelman RM. Characterizing white matter with magnetization transfer and T(2). *Magn Reson Med* 1999;42(6):1128–36. Available from: [https://doi.org/10.1002/\(sici\)1522-2594\(199912\)42:6<1128::aid-mrm18>3.0.co;2-9](https://doi.org/10.1002/(sici)1522-2594(199912)42:6<1128::aid-mrm18>3.0.co;2-9).
- [22] Mossahebi P, Alexander AL, Field AS, Samsonov AA. Removal of cerebrospinal fluid partial volume effects in quantitative magnetization transfer imaging using a three-pool model with nonexchanging water component. *Magn Reson Med* 2015;74(5):1317–26. Available from: <https://doi.org/10.1002/mrm.25516>.
- [23] Yarnykh VL, Yuan C. Cross-relaxation imaging reveals detailed anatomy of white matter fiber tracts in the human brain. *NeuroImage* 2004;23(1):409–24. Available from: <https://doi.org/10.1016/j.neuroimage.2004.04.029>.
- [24] Yarnykh VL. Fast macromolecular proton fraction mapping from a single off-resonance magnetization transfer measurement. *Magn Reson Med* 2012;68(1):166–78. Available from: <https://doi.org/10.1002/mrm.23224>.
- [25] Yarnykh VL. Time-efficient, high-resolution, whole brain three-dimensional macromolecular proton fraction mapping. *Magn Reson Med* 2016;75(5):2100–6. Available from: <https://doi.org/10.1002/mrm.25811>.
- [26] Tabelow K, Balteau E, Ashburner J, Callaghan MF, Draganski B, Helms G, et al. hMRI – a toolbox for quantitative MRI in neuroscience and clinical research. *NeuroImage* 2019;194:191–210. Available from: <https://doi.org/10.1016/j.neuroimage.2019.01.029>.
- [27] Weiskopf N, Suckling J, Williams G, Correia MM, Inkster B, Tait R, et al. Quantitative multi-parameter mapping of R1, PD(\*), MT, and R2(\*) at 3T: a multi-center validation. *Front Neurosci* 2013;7:95. Available from: <https://doi.org/10.3389/fnins.2013.00095>.
- [28] Alsop DC, De Bazelaire C, Garcia M, Duhamel G. Inhomogenous magnetization transfer imaging: a potentially specific marker for myelin. *Proceedings of the 13th annual meeting of ISMRM*. 2005. Miami, FL. Abstract 2224.
- [29] Deloire-Grassin MSA, Brochet B, Quesson B, Delalande C, Dousset V, Canioni P, et al. In vivo evaluation of remyelination in rat brain by magnetization transfer imaging. *J Neurol Sci* 2000;178(1):10–16. Available from: [https://doi.org/10.1016/S0022-510X\(00\)00331-2](https://doi.org/10.1016/S0022-510X(00)00331-2).
- [30] Schmierer K, Scaravilli F, Altmann DR, Barker GJ, Miller DH. Magnetization transfer ratio and myelin in postmortem multiple sclerosis brain. *Ann Neurol* 2004;56(3):407–15. Available from: <https://doi.org/10.1002/ana.20202>.
- [31] Ou X, Sun SW, Liang HF, Song SK, Gochberg DF. The MT pool size ratio and the DTI radial diffusivity may reflect the myelination in shiverer and control mice. *NMR Biomed* 2009;22(5):480–7. Available from: <https://doi.org/10.1002/nbm.1358>.
- [32] Ou X, Sun SW, Liang HF, Song SK, Gochberg DF. Quantitative magnetization transfer measured pool-size ratio reflects optic nerve myelin content in ex vivo mice. *Magn Reson Med* 2009;61(2):364–71. Available from: <https://doi.org/10.1002/mrm.21850>.
- [33] Turati L, Moscatelli M, Mastropietro A, Dowell NG, Zucca I, Erbetta A, et al. In vivo quantitative magnetization transfer imaging correlates with histology during de- and remyelination in cuprizone-treated mice. *NMR Biomed* 2015;28(3):327–37. Available from: <https://doi.org/10.1002/nbm.3253>.
- [34] Gareau PJ, Rutt BK, Karlik SJ, Mitchell JR. Magnetization transfer and multicomponent T2 relaxation measurements with histopathologic correlation in an experimental model of MS. *J Magn Reson Imaging* 2000;11(6):586–95. Available from: [https://doi.org/10.1002/1522-2586\(200006\)11:6<586::aid-jmri3>3.0.co;2-v](https://doi.org/10.1002/1522-2586(200006)11:6<586::aid-jmri3>3.0.co;2-v).

- [35] Blezer EL, Bauer J, Brok HP, Nicolay K, t Hart BA. Quantitative MRI-pathology correlations of brain white matter lesions developing in a non-human primate model of multiple sclerosis. *NMR Biomed* 2007;20(2):90–103. Available from: <https://doi.org/10.1002/nbm.1085>.
- [36] Gass A, Barker GJ, Kidd D, Thorpe JW, MacManus D, Brennan A, et al. Correlation of magnetization transfer ratio with clinical disability in multiple sclerosis. *Ann Neurol* 1994;36(1):62–7. Available from: <https://doi.org/10.1002/ana.410360113>.
- [37] Campi A, Filippi M, Comi C, Scotti G, Gerevini S, Dousset V. Magnetisation transfer ratios of contrast-enhancing and nonenhancing lesions in multiple sclerosis. *Neuroradiology* 1996;38(2):115–19. Available from: <https://doi.org/10.1007/BF00604792>.
- [38] Hiehle Jr. JF, Grossman RI, Ramer KN, Gonzalez-Scarano F, Cohen JA. Magnetization transfer effects in MR-detected multiple sclerosis lesions: comparison with gadolinium-enhanced spin-echo images and non-enhanced T1-weighted images. *AJNR Am J Neuroradiol* 1995;16(1):69–77.
- [39] Filippi M, Rocca MA, Rizzo G, Horsfield MA, Rovaris M, Minicucci L, et al. Magnetization transfer ratios in multiple sclerosis lesions enhancing after different doses of gadolinium. *Neurology* 1998;50(5):1289–93. Available from: <https://doi.org/10.1212/wnl.50.5.1289>.
- [40] van Waesberghe JH, van Walderveen MA, Castelijns JA, Scheltens P, Lycklama à Nijeholt GJ, Polman CH, et al. Patterns of lesion development in multiple sclerosis: longitudinal observations with T1-weighted spin-echo and magnetization transfer MR. *AJNR Am J Neuroradiol* 1998;19(4):675–83.
- [41] Filippi M, Rocca MA, Martino G, Horsfield MA, Comi G. Magnetization transfer changes in the normal appearing white matter precede the appearance of enhancing lesions in patients with multiple sclerosis. *Ann Neurol* 1998;43(6):809–14. Available from: <https://doi.org/10.1002/ana.410430616>.
- [42] Pike GB, Stefano ND, Narayanan S, Worsley KJ, Pelletier D, Francis GS, et al. Multiple sclerosis: magnetization transfer MR imaging of white matter before lesion appearance on T2-weighted images. *Radiology* 2000;215(3):824–30. Available from: <https://doi.org/10.1148/radiology.215.3.r00jn02824>.
- [43] Petrella JR, Grossman RI, McGowan JC, Campbell G, Cohen JA. Multiple sclerosis lesions: relationship between MR enhancement pattern and magnetization transfer effect. *AJNR Am J Neuroradiol* 1996;17(6):1041–9.
- [44] Filippi M, Campi A, Dousset V, Baratti C, Martinelli V, Canal N, et al. A magnetization transfer imaging study of normal-appearing white matter in multiple sclerosis. *Neurology* 1995;45(3 Pt 1):478–82. Available from: <https://doi.org/10.1212/wnl.45.3.478>.
- [45] Traboulsee A, Dehmeshki J, Peters KR, Griffin CM, Brex PA, Silver N, et al. Disability in multiple sclerosis is related to normal appearing brain tissue MTR histogram abnormalities. *Multiple Scler J* 2003;9(6):566–73. Available from: <https://doi.org/10.1191/1352458503ms9580a>.
- [46] Liu Z, Pardini M, Yaldizli Ö, Sethi V, Muhlert N, Wheeler-Kingshott CAM, et al. Magnetization transfer ratio measures in normal-appearing white matter show periventricular gradient abnormalities in multiple sclerosis. *Brain* 2015;138(5):1239–46. Available from: <https://doi.org/10.1093/brain/awv065>.
- [47] Magliozzi R, Howell OW, Reeves C, Roncaroli F, Nicholas R, Serafini B, et al. A Gradient of neuronal loss and meningeal inflammation in multiple sclerosis. *Ann Neurol* 2010;68(4):477–93. Available from: <https://doi.org/10.1002/ana.22230>.
- [48] Brown JW, Pardini M, Brownlee WJ, Fernando K, Samson RS, Prados Carrasco F, et al. An abnormal periventricular magnetization transfer ratio gradient occurs early in multiple sclerosis. *Brain* 2016;140(2):387–98. Available from: <https://doi.org/10.1093/brain/aww296>.
- [49] Brown JW, Prados Carrasco F, Eshaghi A, Sudre CH, Button T, Pardini M, et al. Periventricular magnetisation transfer ratio abnormalities in multiple sclerosis improve after alemtuzumab. *Multiple Scler J* 2020;26(9):1093–101. Available from: <https://doi.org/10.1177/1352458519852093>.
- [50] Vrenken H, Geurts JJ, Knol DL, Polman CH, Castelijns JA, Pouwels PJ, et al. Normal-appearing white matter changes vary with distance to lesions in multiple sclerosis. *AJNR Am J Neuroradiol* 2006;27(9):2005–11.
- [51] Davies GR, Ramió-Torrentà L, Hadjiprocopis A, Chard DT, Griffin CMB, Rashid W, et al. Evidence for grey matter MTR abnormality in minimally disabled patients with early relapsing-remitting multiple sclerosis. *J Neurol Neurosurg Psychiatry* 2004;75(7):998–1002. Available from: <https://doi.org/10.1136/jnnp.2003.021915>.
- [52] Bø L, Vedeler CA, Nyland HI, Trapp BD, Mørk SJ. Subpial demyelination in the cerebral cortex of multiple sclerosis patients. *J Neuropathol Exp Neurol* 2003;62(7):723–32. Available from: <https://doi.org/10.1093/jnen/62.7.723>.
- [53] Khaleeli Z, Cercignani M, Audoin B, Ciccarelli O, Miller DH, Thompson AJ. Localized grey matter damage in early primary progressive multiple sclerosis contributes to disability. *NeuroImage* 2007;37(1):253–61. Available from: <https://doi.org/10.1016/j.neuroimage.2007.04.056>.

- [54] Khaleeli Z, Altmann DR, Cercignani M, Ciccarelli O, Miller DH, Thompson AJ. Magnetization transfer ratio in gray matter: a potential surrogate marker for progression in early primary progressive multiple sclerosis. *Arch Neurol* 2008;65(11):1454–9. Available from: <https://doi.org/10.1001/archneur.65.11.1454>.
- [55] Samson RS, Cardoso MJ, Muhlert N, Sethi V, Wheeler-Kingshott CA, Ron M, et al. Investigation of outer cortical magnetisation transfer ratio abnormalities in multiple sclerosis clinical subgroups. *Multiple Scler J* 2014;20(10):1322–30. Available from: <https://doi.org/10.1177/1352458514522537>.
- [56] Davies GR, Ramani A, Dalton CM, Tozer DJ, Wheeler-Kingshott CA, Barker GJ, et al. Preliminary magnetic resonance study of the macromolecular proton fraction in white matter: a potential marker of myelin? *Multiple Scler J* 2003;9(3):246–9. Available from: <https://doi.org/10.1191/1352458503ms911oa>.
- [57] Levesque IR, Giacomini PS, Narayanan S, Ribeiro LT, Sled JG, Arnold DL, et al. Quantitative magnetization transfer and myelin water imaging of the evolution of acute multiple sclerosis lesions. *Magn Reson Med* 2010;63(3):633–40. Available from: <https://doi.org/10.1002/mrm.22244>.
- [58] Cercignani M, Basile B, Spanò B, Comanducci G, Fasano F, Caltagirone C, et al. Investigation of quantitative magnetisation transfer parameters of lesions and normal appearing white matter in multiple sclerosis. *NMR Biomed* 2009;22(6):646–53. Available from: <https://doi.org/10.1002/nbm.1379>.
- [59] York EN, Thrippleton MJ, Meijboom R, Hunt DPJ, Waldman AD. Quantitative magnetization transfer imaging in relapsing-remitting multiple sclerosis: a systematic review and meta-analysis. *Brain Commun* 2022;4(2):fcac088. Available from: <https://doi.org/10.1093/braincomms/fcac088>.
- [60] McKeithan LJ, Lyttle BD, Box BA, O'Grady KP, Dortch RD, Conrad BN, et al. 7T quantitative magnetization transfer (qMT) of cortical gray matter in multiple sclerosis correlates with cognitive impairment. *NeuroImage* 2019;203:116190. Available from: <https://doi.org/10.1016/j.neuroimage.2019.116190>.
- [61] Lommers E, Guillemain C, Reuter G, Fouarge E, Delrue G, Collette F, et al. Voxel-Based quantitative MRI reveals spatial patterns of grey matter alteration in multiple sclerosis. *Hum Brain Mapp* 2021;42(4):1003–12. Available from: <https://doi.org/10.1002/hbm.25274>.
- [62] Van Obberghen E, Mchinda S, le Troter A, Prevost VH, Viout P, Guye M, et al. Evaluation of the sensitivity of inhomogeneous magnetization transfer (ihMT) MRI for multiple sclerosis. *Am J Neuroradiol* 2018;39(4):634–41. Available from: <https://doi.org/10.3174/ajnr.A5563>.
- [63] Zhang L, Wen B, Chen T, Tian H, Xue H, Ren H, et al. A comparison study of inhomogeneous magnetization transfer (ihMT) and magnetization transfer (MT) in multiple sclerosis based on whole brain acquisition at 3.0 T. *Magn Reson Imaging* 2020;70:43–9. Available from: <https://doi.org/10.1016/j.mri.2020.03.010>.
- [64] Smith SA, Golay X, Fatemi A, Jones CK, Raymond GV, Moser HW, et al. Magnetization transfer weighted imaging in the upper cervical spinal cord using cerebrospinal fluid as intersubject normalization reference (MTCFSF imaging). *Magn Reson Med* 2005;54(1):201–6. Available from: <https://doi.org/10.1002/mrm.20553>.
- [65] Zackowski KM, Smith SA, Reich DS, Gordon-Lipkin E, Chodkowski BA, Sambandan DR, et al. Sensorimotor dysfunction in multiple sclerosis and column-specific magnetization transfer-imaging abnormalities in the spinal cord. *Brain* 2009;132(5):1200–9. Available from: <https://doi.org/10.1093/brain/awp032>.
- [66] Battiston M, Grussu F, Ianus A, Schneider T, Prados F, Fairney J, et al. An optimized framework for quantitative magnetization transfer imaging of the cervical spinal cord in vivo. *Magn Reson Med* 2018;79(5):2576–88. Available from: <https://doi.org/10.1002/mrm.26909>.
- [67] Smith AK, By S, Lyttle BD, Dortch RD, Box BA, McKeithan LJ, et al. Evaluating single-point quantitative magnetization transfer in the cervical spinal cord: application to multiple sclerosis. *Neuroimage Clin* 2017;16:58–65. Available from: <https://doi.org/10.1016/j.nicl.2017.07.010>.
- [68] Taso M, Girard OM, Duhamel G, Le Troter A, Feiweiwei T, Guye M, et al. Tract-specific and age-related variations of the spinal cord microstructure: a multi-parametric MRI study using diffusion tensor imaging (DTI) and inhomogeneous magnetization transfer (ihMT). *NMR Biomed* 2016;29(6):817–32. Available from: <https://doi.org/10.1002/nbm.3530>.
- [69] Trip S, Schlottmann P, Jones S, Li W-Y, Garway-Heath D, Thompson A, et al. Optic nerve magnetization transfer imaging and measures of axonal loss and demyelination in optic neuritis. *Multiple Scler J* 2007;13(7):875–9. Available from: <https://doi.org/10.1177/1352458507076952>.
- [70] Smith AK, Dortch RD, Dethrage LM, Lyttle BD, Kang H, Welch EB, et al. Incorporating dixon multi-echo fat water separation for novel quantitative magnetization transfer of the human optic nerve in vivo. *Magn Reson Med* 2017;77(2):707–16. Available from: <https://doi.org/10.1002/mrm.26164>.